

Articles

Quadruplex-Interactive Agents as Telomerase Inhibitors: Synthesis of Porphyrins and Structure–Activity Relationship for the Inhibition of Telomerase

Dong-Fang Shi,[†] Richard T. Wheelhouse,^{†,‡} Daekyu Sun,[§] and Laurence H. Hurley^{*,†,||}

College of Pharmacy, University of Texas at Austin, Austin, Texas 78712, The School of Pharmacy, The University of Bradford, Bradford BD7 1DP, United Kingdom, Institute for Drug Development, 14960 Omicron Drive, San Antonio, Texas 78245, Arizona Cancer Center, 1515 North Campbell Avenue, Tucson, Arizona 85724, and College of Pharmacy, The University of Arizona, Tucson, Arizona 85721

Received June 1, 2001

The cationic porphyrin 5,10,15,20-tetra-(*N*-methyl-4-pyridyl)porphyrin (TMPyP4) binds to quadruplex DNA and is thereby an inhibitor of human telomerase (Wheelhouse et al. *J. Am. Chem. Soc.* **1998**, *120*, 3261–3262). Herein the synthesis and telomerase-inhibiting activity of a wide range of analogues of TMPyP4 are reported, from which rules for a structure–activity relationship (SAR) have been discerned: (1) stacking interactions are critical for telomerase inhibition, (2) positively charged substituents are important but may be interchanged and combined with hydrogen-bonding groups, and (3) substitution is tolerated only on the *meso* positions of the porphyrin ring, and the bulk of the substituents should be matched to the width of the grooves in which they putatively lie. This SAR is consistent with a model presented for the complexation of TMPyP4 with human telomeric quadruplex DNA.

Introduction

Quadruplex DNA presents a target of considerable current interest in DNA-directed drug design.^{1–8} The initial interest in quadruplexes emerged from their involvement in telomeres and in the regulation of telomerase activity, but a wider biological significance for quadruplex DNA is now becoming apparent. For example, there is evidence for a role in the regulation of gene expression following the discovery of putative quadruplex-forming sequences located in the promoter regions of a number of genes, including the *c-MYC* oncogene⁹ and insulin.¹⁰ The potential to form DNA quadruplexes has also been demonstrated for the abnormal chromosomal DNA present in patients suffering from Friedreich's ataxia, fragile X syndrome, and Huntington's disease.^{11–13} Furthermore, the existence and significance of quadruplex formation *in vivo* are demonstrated by the existence of proteins that either specifically bind to or promote the folding of quadruplex structures.^{14–17}

Telomerase is expressed in over 90% of tumor cell lines but in only a few, specialized, normal healthy cells.¹⁸ The link to controlling the growth of tumor cells is now established: expression of a mutant, nonfunctional human telomerase results in the reduction of chromosomal telomere length and death of tumor cells.¹⁹

Thus, telomerase inhibition represents a potentially highly selective target for anticancer drug design.¹⁸ For an excellent recent review of the relationship among telomeres, telomerase, telomerase inhibitors, and cancer, see de Lange and Jacks.²⁰

One effective strategy for the design of telomerase inhibitors has been the targeting of its DNA substrate. At the extreme 3'-termini of the telomeres there are regions of single-stranded DNA, formed because of a limitation of the DNA polymerization mechanism, the *end replication problem*.²¹ In humans the single-stranded overhang may be up to 160 bases long.²² A property of G-rich, single-stranded DNA is that it can fold into a four-stranded structure assembled around a core stack of guanines arranged in almost-planar, hydrogen-bonded tetrads. Ionic conditions that favor quadruplex formation have been shown to inhibit telomerase,²³ while small molecules that stabilize or promote the formation of quadruplex also show inhibitory activity.^{24–27} Thus, quadruplexes have an important role in controlling telomerase activity, and thereby tumor growth, and possibly in other conditions connected to the aging process.

The number of known small-molecule quadruplex ligands has been relatively small^{2–5,26} until recently and can be divided into two classes: putative groove binders (carbocyanine dyes²⁸) and extended aromatic chromophores. The latter category includes cationic porphyrins (e.g., TMPyP4),²⁵ anthraquinones (e.g., **1**),²⁴ and related tricyclic²⁹ or tetracyclic systems,³⁰ the perylene **2**,³¹ ethidium **3**,³² ethidium conjugates,³³ pentacyclic methylacridinium salt,³⁴ and quinoline-based ligands.³⁵

* To whom correspondence should be addressed. Phone: (520) 626-5622. Fax: (520) 626-5623. E-mail: hurley@pharmacy.arizona.edu.

[†] University of Texas at Austin.

[‡] The University of Bradford.

[§] Institute for Drug Development.

^{||} Arizona Cancer Center and The University of Arizona.

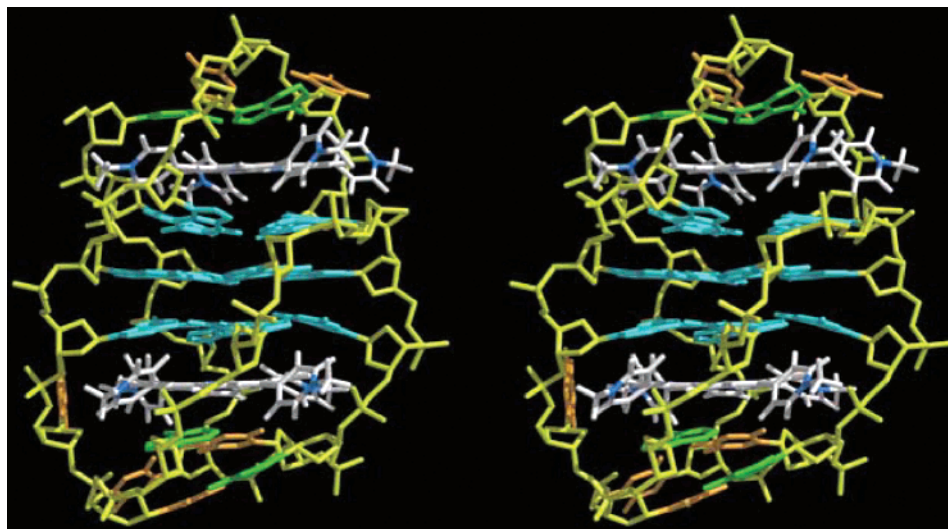
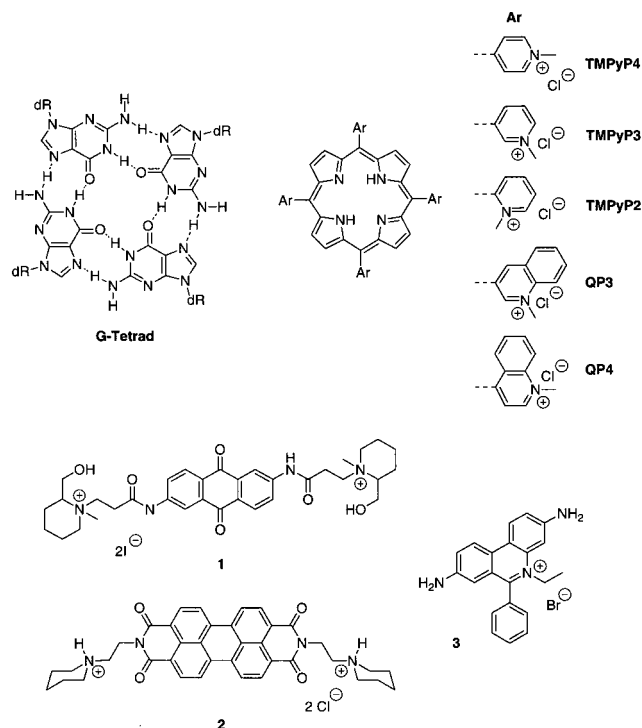


Figure 1. Minimized model of a 2:1 complex between TMPyP4 and the human d(AG₃[T₂AG₃]₃) quadruplex. The sugar phosphate backbone is colored in yellow, G in cyan, A in green, T in orange, and the porphyrin in blue and white.

The common structural feature of all these compounds is an extended planar chromophore that can stack on, or intercalate, the G-tetrads at the core of DNA quadruplexes in such a manner that any pendant groups may fall into the grooves of the quadruplex, with the cationic moieties directed toward the backbone phosphates. Ligand interaction with quadruplex structures is accompanied by stabilization of the quadruplex and consequent inhibition of telomerase. The best of the porphyrins³⁶ and anthraquinones²⁶ show 50% telomerase inhibition (IC₅₀) using a standard assay at 1–25 μ M; in vitro studies have shown that the cationic porphyrin TMPyP4 is able to shorten telomeres, induce a delayed cell crisis (2–4 weeks), and induce apoptosis.³⁷



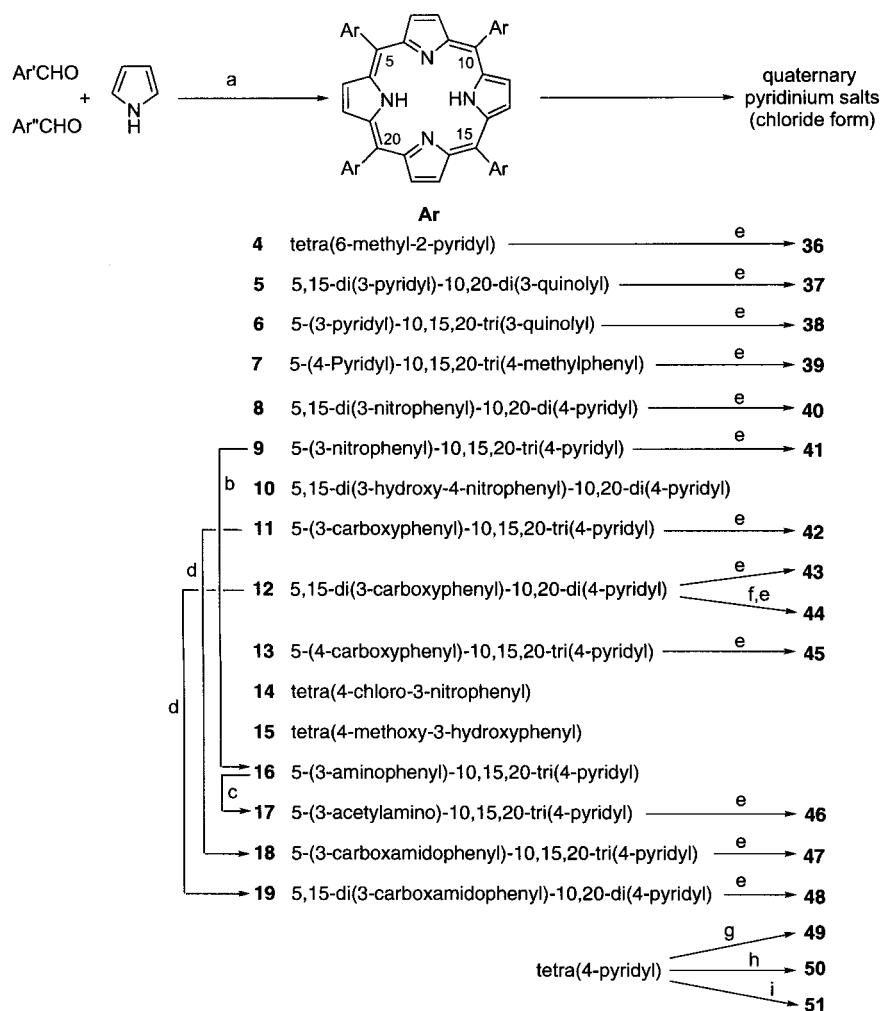
We have previously reported²⁵ that TMPyP4 is an effective inhibitor of human telomerase in a cell-free assay. Herein the synthesis and telomerase-inhibiting

activity of a wide range of analogues of TMPyP4 are reported, from which SAR rules may be discerned that are consistent with a model presented for the complexation of TMPyP4 with human telomeric quadruplex DNA.

Results and Discussion

Lead Identification and Molecular Modeling. A consideration of the relative dimensions of TMPyP4 and the G-tetrads that stabilize quadruplex DNA suggested that the two were of appropriate size for complexation, stabilized by favorable stacking interactions. Indeed, the crystal structure of a complex of TMPyP4 with a short DNA duplex has two notable features: while the porphyrin ring does stack with the DNA bases, it is too large to fully intercalate so that only about half of the porphyrin ring is inserted into the duplex; furthermore, this is accompanied by considerable disruption of the DNA helical structure adjacent to the *hemi-intercalation* site.³⁸ A recent solution structure³⁹ is at variance with the crystal structure in that true intercalation is claimed; however, the size of the porphyrin remains much larger than the cross-section through a duplex. Spectrophotometric experiments with a variety of DNA quadruplex sequences^{25,40} have unambiguously indicated stacking interactions between porphyrin and DNA, accompanied by stabilization of the quadruplexes to thermal denaturation.

A model of how TMPyP4 might bind to the human telomeric quadruplex is shown in Figure 1. The solution structure of a 22-base oligonucleotide derived from the human telomere sequence d(AG₃[T₂AG₃]₃) has been solved,⁴¹ and it consists of a single looped strand that is stabilized by a core of stacked G-tetrads. Using coordinates from the solution structure of the quadruplex and crystal structure of the porphyrin, and stoichiometry determined experimentally (see ref 25, Supporting Information), a minimized model of the 2:1 TMPyP4–d(AG₃[T₂AG₃]₃) complex was built. It was found that the quadruplex could accommodate porphyrins above and below the tetrads at the core of the complex with very little distortion. The porphyrins lay stacked on the tetrads and could be orientated so that

Scheme 1^a


^a Reagents and conditions: (a) EtCO₂H/ Δ ; (b) SnCl₂/HCl/room temperature; (c) Ac₂O/Et₃N/CHCl₃/ Δ ; (d) CDI/THF/ Δ /NH₄OH; (e) (i) MeI/CHCl₃/ Δ , (ii) Dowex 1X2-200; (f) CDI/THF/ Δ /BrCH₂CH₂NH₂·HBr/Et₃N; (g) (i) EtI/CHCl₃/ Δ , (ii) Dowex 1X2-200; (h) (i) BrCH₂OAc/CHCl₃/ Δ , (ii) Dowex 1X2-200; (i) (i) ICH₂CH₂OH/CHCl₃/ Δ , (ii) Dowex 1X2-200.

the positively charged groups were directed into the grooves toward the sugar–phosphate backbone. The *N*-methylpyridinium rings were tilted from the plane of the porphyrin to follow the twist of the grooves. Following minimization, the porphyrins appeared slightly offset from the center of the tetrads, a result that is probably due to the threading distance of the porphyrins being slightly smaller than the cross-section of the tetrads. A more thorough molecular modeling study with TMPyP4 and d(AG₃[T₂AG₃]₃) is reported in ref 42.

The binding site of TMPyP4 on fold-over quadruplexes has been controversial. Although we have presented extensive photochemical cleavage evidence that porphyrins lie stacked externally on the terminal faces of the G-tetrad core rather than truly intercalated,^{25,43} a subsequent spectrophotometric, calorimetric, and modeling study⁴⁴ has proposed that TMPyP4 is actually able to truly intercalate the tetrads of quadruplex DNA sequences. Our experience with other drugs, notably the perylene **2**, which remains the only compound for which an unambiguous binding site has been determined,³³ in the absence of unequivocal data for TMPyP4 (NMR or X-ray), leads us to favor the externally stacked site. In addition, we have recently reconfirmed the favored outside binding site for TMPyP4.⁴² The SAR data

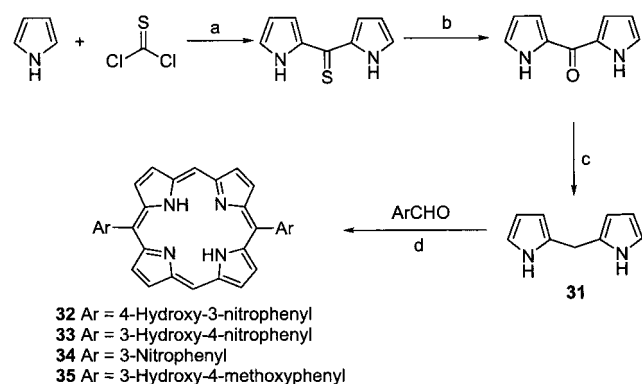
presented herein may be interpreted in a manner consistent with either the intercalation or externally stacked model.

Synthesis. Porphyrins that were not commercially available were synthesized by variations on established methods.⁴⁵ Thus, an aryl aldehyde or an appropriate mixture of aryl aldehydes was condensed with pyrrole to give the *meso*-substituted porphyrins **4**–**19**, as shown in Scheme 1; the products were separated by flash column chromatography. While the yields were poor, this approach was feasible where the aldehydes were readily and cheaply available.

Reduction of nitroporphyrin **9** with tin chloride⁴⁶ in 6 M HCl gave aminoporphyrin **16**; in contrast, when **9** was treated with tin chloride in EtOH, a tin(II) complex of **16** was obtained. Acetylation of **16** was achieved by reaction with acetic anhydride in the presence of triethylamine to give amide **17**. Porphyrin **11** was converted to its amide **18** by treatment with carbonyldiimidazole and aqueous ammonia solution. Similarly, porphyrin **19** was obtained from **12**.

Routes for the preparation of *meso*-pyridylporphyrins bearing furan and thiophene substituents on the pyridine rings are illustrated in Scheme 2. Reduction of 3-bromopyridine-5-carboxylic acid to the alcohol **20** was

Scheme 3^a



^a Reagents and conditions: (a) (i) ether/benzene/0 °C, (ii) 80% MeOH/room temperature; (b) 95% EtOH/KOH/5% H₂O₂; (c) NaBH₄/95% EtOH/morpholine/Δ; (d) (i) TFA/CH₂Cl₂, (ii) chloranil/Δ.

thesis of 5,15-diarylporphyrins was attempted as outlined in Scheme 3. 2,2'-Dipyrrylmethane (**31**) was synthesized in three steps via 2,2'-dipyrryl thioketone and 2,2'-dipyrryl ketone from pyrrole and thiophosgene in 65% overall yield by a modification of the literature method.^{50,51} Condensation of **31** with aryl aldehydes following the method of Mankra and Lawrence⁵² gave the *trans*-disubstituted porphyrins **32–35** in good yields. Disappointingly, condensation with pyridaldehydes under similar reaction conditions failed to yield 5,15-dipyridyl-substituted porphyrins.

Quaternization of the free bases of pyridyl- and quinolyl-substituted porphyrins was accomplished by reaction with alkyl iodides in chloroform or a mixture of chloroform and nitromethane.⁵³ The salts precipitated and were converted to the chloride form by ion exchange on a large pore size Dowex 1 resin to give the porphyrin salts **36–51**, which were assayed against telomerase.

Telomerase Inhibition Data. Telomerase inhibition was assessed by measuring the activity against telomerase from an HeLa cell extract using a primer extension assay.⁵⁴ A 5'-biotinylated primer consisting of three telomeric repeats was employed and the incorporation of ³²P-labeled GTP measured. To facilitate screening of large numbers of compounds, the porphyrin concentration was fixed at 25 μM, and TMPyP4 and QP3 were included as controls in each experiment. Data are presented in Tables 1–7 as the percentage of inhibition of telomerase relative to the telomerase activity measured in the porphyrin-free control (0%). Compounds are grouped to illustrate particular phenomena of the SAR. Selected compounds were additionally assayed over a range of concentrations to determine IC₅₀ values (Table 8) and to investigate mechanistic aspects of telomerase inhibition (Figure 2).

Inhibition of telomerase in this cell-free assay can be the result of one or more interactions between the porphyrin and DNA. TMPyP4 gives a classical pattern typical of G-quadruplex interaction; i.e., inhibition takes place only after extension of the 18-mer primer by telomerase to a 28-mer, which provides four repeats of TTAGGG, the minimum sufficient to form a G-quadruplex structure.²⁴ However, other interactions that result from binding to the single-stranded primer or photocleavage of the primer can also result in apparent inhibition of telomerase activity. To avoid photocleav-

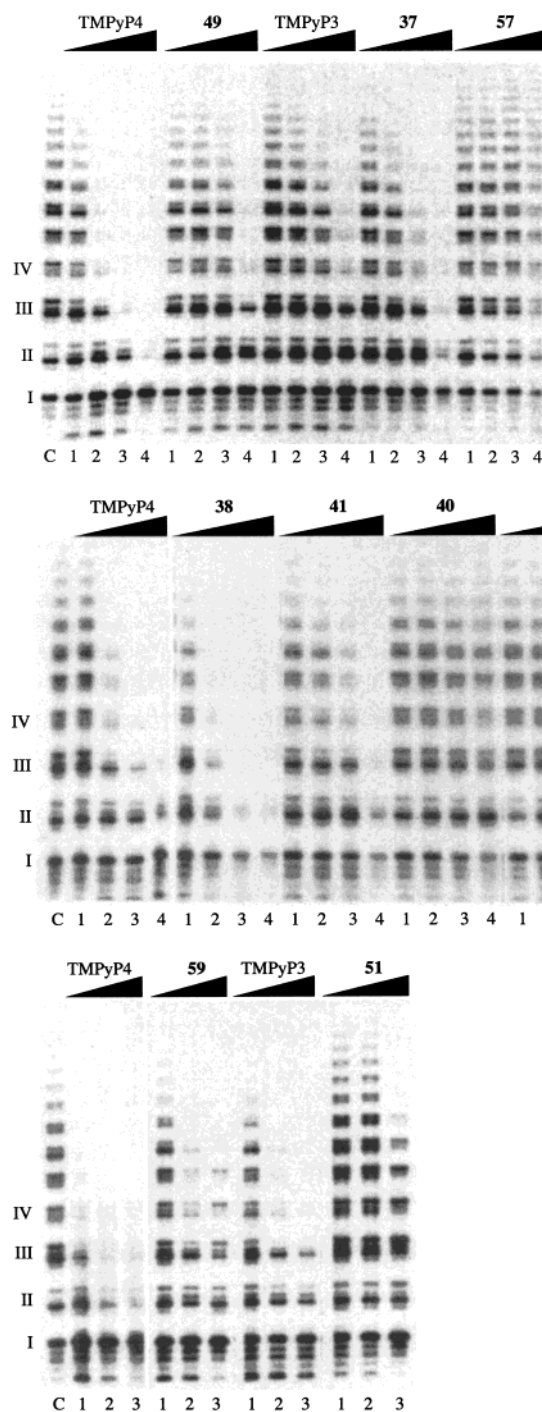


Figure 2. Gels illustrating apparent inhibition of telomerase by different mechanisms (see Table 8).

age, solutions were protected from light. The pattern of the telomerase extension ladder is indicative of whether nonspecific inhibition or interaction with the G-quadruplex is responsible for the apparent telomerase inhibition. Examples of telomerase extension ladders where nonspecific inhibition occurs due to binding to single-stranded DNA are shown in Figure 2. In our early experiments there was confusion over interpretation of the gels where photocleavage was superimposed on telomerase inhibition; accordingly, we report the value for the IC₅₀ of TMPyP4 as 8 ± 2 μM.

A further complication in interpretation of the results is discerning whether the porphyrin binds to a pre-

Table 1. Telomerase Inhibition by Metal Complexes of TMPyP4^a

porphyrin	metal ion	geometry	% inhibition (25 μ M)
TMPyP4	H2		88
	Zn(II)	py	88
	Co(II)		83
	Fe(III)	oh	63
	Ni(II)	sqpl \leftrightarrow oh	42
	Mn(III)	oh	37
	Cu(II)	sqpl	75
	Mg(II)	oh	42
	Pt(II)	sqpl	69
	Pd(II)	sqpl	41
QP3	2H		56

^a All other ligands were chloride. Abbreviations: sqpl, square planar; oh, octahedral; py, pyramidal.

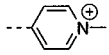
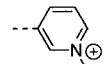
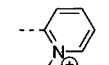
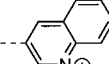
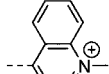
formed quadruplex structure or whether binding of porphyrin to single-stranded DNA facilitates G-quadruplex formation, as has been shown for the perylene **2**.⁵⁵ We have recently shown that TMPyP4 has a modest effect on facilitation of intramolecular quadruplex formation, and thus the effects we observe are most likely related to binding to the preformed G-quadruplex structure (M.-Y. Kim and L. H. Hurley, unpublished results).

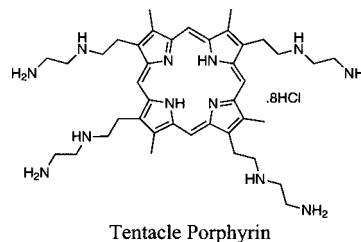
The results of a series of telomerase inhibition experiments using compounds selected from those listed in Tables 1–7 (and in the Supporting Information) are shown in Figure 2 and in Table 8. In each case, using a range of concentrations (3.1–25 μ M) of each cationic porphyrin, the IC₅₀ and pattern of inhibition were used to predict the mechanism of telomerase inhibition (i.e., interaction with the G-quadruplex structure or primer, or mixed). While most of the compounds showed a selective G-quadruplex interaction similar to that of TMPyP4, some compounds showed interactions with both primer and G-quadruplex structures (**37**, **38**, **44**, and **51**), and one showed little evidence of G-quadruplex interaction, instead showing primer binding (**57**). Most compounds were less potent than TMPyP4 in telomerase inhibition, with the possible exception of the triquinolyl **38**.

Structure–Activity Relationships. Groups of compounds were designed to determine the effects on telomerase inhibitory activity by variations on the basic TMPyP4 structure: i.e., coordinated metal ion, number of charges on the *meso* substituents, disposition of charges around the porphyrin ring, position of the charged group on the *meso* substituents, bulk of the substituents, and effects of different quaternizing groups. A wide range of natural porphyrins and their close analogues were also investigated. The results are presented in Tables 1–7 (and in the Supporting Information).

Stacking Interactions Are Crucial for Telomerase Inhibition. The data in Table 1 show the effects of coordination to different metal ions on the inhibition of telomerase by TMPyP4. Across the first-row transition metals, a general relationship is apparent between the coordination chemistry of the metal ion and the degree of telomerase inhibition. Those complexes where the porphyrin offered an unhindered face for stacking were the better inhibitors, that is, the square planar Cu(II) complex (75% inhibition at 25 μ M) and pyramidal

Table 2. Dependence of Telomerase Inhibition on the Ability of the Porphyrin to Stack with G-Tetrads

Porphyrin	<i>meso</i> -Ar	% Inhibition (25 μ M)
TMPyP4		66
TMPyP3		54
TMPyP2		0
QP3		14
QP4		0
Tentacle	n/a	0



Zn(II) (88%). In contrast, octahedral complexes, in which the metal ion carried two strongly bound axial ligands that would pose a block to stacking interactions, were generally less active, for example, Mn(III) (37%) and Mg(II) (42%). In the complexes of TMPyP4 with second- and third-row transition-metal ions and lanthanides (see the Supporting Information), the larger ions do not fit in the cavity but lie above the plane of the porphyrin ring so that even the formally square planar Au(III) complex has an impediment to stacking and was found to be a poor inhibitor (23%) of telomerase (Table 9 in the Supporting Information). This situation was exacerbated in the lanthanide complexes.

It should be noted that some of the free porphyrins exhibit DNA photocleavage activity, a trait not desirable in a telomerase inhibitor intended for clinical use. However, this activity may be modulated by the choice of complexed metal ion: for example, the Cu(II) ion, with its unpaired d-electron, is able to quench the excited state of the porphyrin and so reduce its photocleavage activity.⁵⁶ The data in Table 1 indicate that Cu(II) complexes may be used in drug preparations without detriment to the telomerase inhibitory activity of the porphyrin.

Conclusive evidence of the importance of stacking interactions to the process by which telomerase is being inhibited comes from the data in Table 2. When a porphyrin bears *meso*-aryl substituents, the porphyrin and substituent aryl rings do not lie in the same plane, so there is a twist about the bond between the porphyrin and aryl rings (observe the porphyrin and its pyridyl

Table 3. Effects of Substituent Bulk

Porphyrin	5-Ar	10-Ar	15-Ar	20-Ar	% Inhibition (25 μ M)
TMPyP4					60
TMPyP3					50
37					80
38					90
QP3					28

substituents in the model, Figure 1). However, where the *meso*-aryl substituent carries a group other than a hydrogen atom on the 2-position, the 2-substituent lies partly over the face of the porphyrin, posing a block to stacking. Steric hindrance prevents any rotation about the bond between the rings to facilitate exposure of the porphyrin surface, a situation similar to the formation of atropisomers in analogous biaryl systems. Thus, in the case of TMPyP2, the *N*-methyl groups partially obscure the faces of the porphyrin, and stacking interactions are not possible. The consequence of this structural feature for telomerase inhibition is demonstrated by the data in Table 2. As the *N*-methyl group of the pyridine was moved from the 4-position to the 3- and 2-positions, there was a dramatic loss of telomerase inhibition for the 2-pyridyl analogue (66%, 54%, and 0%, respectively). This pattern of activity has also been documented in duplex DNA photocleavage assays where binding is dependent on intercalation.⁵⁶ A similar situation pertained for the quinolyl series QP3 and QP4 where the 4-quinolyl compound, which places the fused benzo ring over the face of the porphyrin, was the least active of all the tetracationic compounds tested, even at higher concentrations.

Substitution at the β -Positions of the Pyrrole Rings Is Not Tolerated. The inactivity of the tentacle porphyrin (Table 2) is, at first sight, a little surprising. The polyamine side chains give the compound a net charge of 8+, so good DNA affinity would be expected. However, attempts to construct a stacked model of this porphyrin in quadruplex DNA proved fruitless. It was impossible to orient the porphyrin stacked so that the polycationic chains were directed into the grooves and toward phosphate groups without encountering severe steric clashes with the sugar-phosphate backbone of the DNA. It was therefore concluded that substitution at the β -positions of the pyrrole rings could not be accommodated within the complex with quadruplex DNA. This conclusion was reinforced by an extensive selection of naturally occurring compounds, bearing a

range of substituents at the β -positions of the pyrrole rings, which showed little activity against telomerase (Supporting Information).

Substituent Bulk Is an Important Determinant of Telomerase Inhibition. The grooves of the intramolecular DNA quadruplex are not all the same size:⁴¹ a very narrow groove lies opposite a wide groove, with two intermediate-width grooves between. Therefore, a series of compounds was designed to investigate the importance of matching the bulk of the *meso* substituents around the porphyrin to the width of the grooves in which they might lie when stacked on quadruplex DNA. The data shown in Table 3 demonstrate the effect of varying the number of *N*-methylpyridyl and *N*-3-methylquinolyl substituents around the porphine nucleus (**37** and **38**). Thus, when all four groups were small (TMPyP4, TMPyP3), telomerase inhibition of 50–60% was observed. At the other extreme, when all four groups were large (*N*-methylquinol-3-yl, QP3), only 28% inhibition occurred. However, replacing only one of the *N*-methylquinol-3-yl groups of QP3 with *N*-methylquinol-3-yl, **38**, resulted in activity equivalent to or greater than that of TMPyP4. This can be rationalized in terms of the smaller pyridyl group better fitting into the minor groove of the quadruplex and therefore allowing more effective binding of the porphyrin to its target.

Positive Charge Is Required for Telomerase Inhibition. Many DNA-targeted drugs rely on simple ionic interactions to confer intrinsic DNA binding affinity. Since DNA is polyanionic, the number of positive charges on a ligand would be expected to have significant consequences for ligand–DNA interaction; in addition, the disposition of these charges around the ligand may be important. The compounds presented in Table 4 were chosen to investigate the effect of changing the number and disposition of positive charges around the porphyrin ring on telomerase inhibition. In the 4-pyridyl series (**39** and **52–56**), the general trend was that telomerase inhibition was charge-dependent such that

Table 4. Effect of Varying the Number and Disposition of Charged Groups around the Porphyrin Nucleus

Porphyrin	5-Ar	10-Ar	15-Ar	20-Ar	Charge	% Inhibition (25 μ M)
TMPyP4					4+	62
52				Ph	3+	15
53		Ph		Ph	2+ trans	30
54			Ph	Ph	2+ cis	20
55		Ph	Ph	Ph	1+	34
39		4-Tol	4-Tol	4-Tol	1+	31
56	Ph	Ph	Ph	Ph	0	7
QP3					4+	37

the tetracationic compounds were the better inhibitors and the uncharged analogue was inactive. However, some results, such as the greater activity of the 1+ species (**55**, 34%) versus the 3+ species (**52**, 15%), cannot be rationalized purely on the basis of charge effects. The disposition of charges also appeared to be important since the isomeric 2+ analogues showed different activities (30% *trans*, **53**; 20% *cis*, **54**). A similar pattern of activities was determined for the 3-pyridyl series (Supporting Information).

Substituents on the *N*-Positions of the Pyridine Rings Do Not Affect Activity Unless There Is Charge Neutralization. The compounds listed in Table 5 were used to investigate the effect of different pyridine *N*-alkyl substituents on telomerase inhibition. In all cases where the positive charge was maintained, there was little variation in telomerase inhibitory activity across the series methyl (TMPyP4), ethyl (**49**), hydroxyethyl (**51**), and acetoxymethyl (**50**). The two compounds resulting in zwitterions and hence zero net charge, **52** and **53**, showed no activity. The same trend was apparent for the 3-pyridyl series (Supporting Information).

A Combination of H-Bonding and Charged Substituents Improves Telomerase Inhibition. The results in Table 6 test the concept that uncharged compounds bearing appropriate hydrogen-bonding groups may be telomerase inhibitors. This idea was developed further where charged and hydrogen-bonding substituents were combined around the porphyrin ring (Table 7). Substitution of neutral but H-bonding substituents for the charged pyridinium species does not improve telomerase inhibitory activity (no better than 55% telomerase inhibition). However, a combination of two

Table 5. R Groups

Porphyrin	<i>meso</i> -Ar	% Inhibition (25 μ M)
TMPyP4		67
49		55
50		15
51		55
52		0
53		14
QP3		32

cationic and two hydrogen-bonding substituents gave compounds with good activity (**40**, **41**, **43**, **44**, and **46–48**). The exception to this trend was the carboxy compounds (**42** and **45**), where ionization of the carboxylate at physiological pH would be expected to reduce the intrinsic electrostatic affinity of the compounds for DNA. The particular activity (95%) of the bromoethyl-

Table 6. Effect of Uncharged Hydrogen-Bonding Groups

Porphyrin	5-Ar	10-Ar	15-Ar	20-Ar	% Inhibition (25 μ M)
TMPyP4					60
QP3					28
14					insoluble
15					50
32		H		H	55
34		H		H	insoluble

Table 7. Combination of Charged and Hydrogen-Bonding Groups

Porphyrin	5-Ar	10-Ar	15-Ar	20-Ar	% Inhibition (25 μ M)
TMPyP4					60
QP3					30
40					70
41					85
42					18
43					48
44					95
45					10
46					55
47					55
48					85

amide compound **44** may be due to its potential to alkylate or cross-link DNA.

Rational Design of New *meso* Substituents. Given the model of the porphyrins stacking on the G-tetrads that is consistent with all the SARs described above and the significance of electrostatic and hydrogen-bonding interactions, compound **57** was designed and synthesized (see Scheme 2). The *meso*-pyridyl substituents all carry a positive charge in the 3-position and are elaborated further by the addition of a furan ring. The

furan rings were crucially located so that, in the complex with the tetraplex, the oxygen atoms could be oriented to form hydrogen bonds with the guanine N(2)H positions located on the edges of the G-tetrads immediately adjacent to the stacking site. While an increase in telomerase inhibitory activity was duly seen (86% at 25 μ M compared with 60% for TMPyP4 and 30% for QP3; unpublished results), upon examination of the pattern of inhibition (Figure 2A) this compound provided a telomere elongation ladder that was more consistent

Table 8. Telomerase IC₅₀ of Compounds from Figure 2

Figure 2A		
compound ^a	IC ₅₀ (μM)	mechanism ^b
TMPyP4	6.25	G4
49	25	G4
TMPyP3	25	G4
37	10	mixed
57	8	primer
Figure 2B		
compound ^a	IC ₅₀ (μM)	mechanism ^b
TMPyP4	8	G4
38	5	mixed
41	12	G4
40	25	G4
44	15	mixed
Figure 2C		
compound ^a	IC ₅₀ (μM)	mechanism ^b
TMPyP4	10	G4
59	20	G4
TMPyP3	12	G4
51	30	mixed

^a Numbers refer to compounds in Tables 1–7. ^b G4: interaction with G-quadruplex. Primer: interaction with primer. Mixed: interaction with G-quadruplex and primer.

with primer interaction than specific interaction with a G-quadruplex structure, even though it was equivalent to TMPyP4 in inhibition of telomerase. The interaction with the primer may mask the G-quadruplex interaction and more potent telomerase inhibition.

Conclusions

Cationic porphyrins have been identified that are effective inhibitors of human telomerase, with the best exhibiting cell-free IC₅₀ values in the range 5–25 μM. It is important to note that when using the more familiar TRAP assay the telomerase inhibitory concentrations of cationic porphyrins are about 10 times lower, i.e., IC₅₀ in the submicromolar range (C. Grand and L. H. Hurley, unpublished results). From data pertaining to a wide range of analogues, a basic SAR has been determined: (1) the face of the porphyrin must be available for stacking, (2) the positively charged substituents are important but may be interchanged and combined with hydrogen-bonding groups, and (3) substitution is tolerated only on the *meso* positions of the porphyrin, and the size of the substituents should be matched to the width of the grooves in which they putatively lie. These factors are all consistent with a model in which the porphyrins stack externally on the G-tetrads of the quadruplex, placing the *meso* substituents in each of the four grooves.

The cationic porphyrins represent a very promising class of compounds for the development of clinical telomerase inhibitors. For a compound to be useful, it must have a significant therapeutic window between its activity against telomerase and the onset of cytotoxic effects. This is clearly so with the porphyrins; for example, TMPyP4 has a cell-free telomerase IC₅₀ value of about 8 μM, and telomere shortening is noted with concentrations between 1 and 5 μM,³⁷ but its cytotoxic IC₅₀ against a panel of normal and transformed breast and prostate cell lines is in the range 50–200 μM.²⁷ Furthermore, evidence exists for the uptake and concentration of TMPyP4 in the nuclei of cells grown in

culture^{27,57} and for its accumulation in tumor tissue in mice.⁵⁸ Thus, the cationic porphyrins have a number of properties that render them attractive candidates for development as telomerase inhibitors for the treatment of patients with cancer. The data presented herein lay the foundations for a program of drug development to achieve the dual aims of efficacy and selectivity *in vivo*. Furthermore, we have found that cellular effects following administration of TMPyP4 may be related not only to telomerase inhibition but also to disruption of other G-quadruplex structures,^{27,59} leading to more rapid onset of telomere shortening, chromosomal instability, cell crisis, apoptosis,³⁷ and other consequences of telomere malfunction (e.g., anaphase bridges) that cannot be accounted for by a mechanism invoking telomerase inhibition and concomitant telomere shortening alone.

Experimental Section

Molecular Modeling. Models were built using the SYBYL package (Tripos Inc., St. Louis, MO). Coordinates for the DNA quadruplex⁴¹ and TMPyP4³⁸ were obtained from the Brookhaven Protein Data Bank. Hydrogen-bonding constraints were added to the G-tetrads, and torsional constraints were set to maintain the planarity of the porphyrins; charges on the porphyrin tetracation were calculated in MOPAC. Porphyrins were inserted above and below the G-tetrads, and the complex was allowed to minimize using Kollman charges, the Tripos force field, and the conjugate gradient. After 100 iterations the porphyrins were replaced, and the minimization was repeated for 500 iterations to a terminal gradient of 0.05 kcal/mol.

Synthesis. 5,10,15,20-Tetra(*N*-[2-hydroxyethyl]-4-pyridyl)-porphine chloride (**51**)⁵³ and 2,2'-dipyrrylmethane (**31**)^{49,51} were prepared according to published procedures. Porphyrins not described in the synthetic section were obtained from Mid-century, Posen, IL. Melting points are uncorrected. Analytical thin-layer chromatography was performed on silica-coated plastic plates (silica gel 60 F-254, Merck) and visualized under multiband UV-254/366 nm light. Preparative separations were performed by flash column chromatography⁶⁰ on 60 mesh silica gel. ¹H NMR spectra were acquired on a Bruker AC250 spectrometer. Low-resolution mass spectra were obtained with either a Finnigan-MAT 4023 or a Bell and Howell 21-491 instrument, fast atom bombardment mass spectra (FAB MS) were determined with a Finnigan-MAT TSQ-70 instrument, and high-resolution mass spectra were recorded on a Bell and Howell 21-110B instrument.

General Method A: Preparation of 5,10,15,20-Tetra-substituted Porphyrins.^{45,61} A mixture of pyrrole (10 mmol) and 1 equiv of the appropriate aryl carboxaldehyde or a mixture of aryl carboxaldehydes in 40 mL of propionic acid was stirred at reflux in air for 1 h. The solvent was evaporated under high vacuum, and the products were purified by flash column chromatography.

General Method B: Preparation of 5,15-Disubstituted Porphyrins.⁵² **31** (0.54 mmol) and 1 equiv of aryl aldehyde were dissolved in dry dichloromethane (60 mL) under argon, and one drop of trifluoroacetic acid was added. The mixture was stirred under argon at room temperature for 18 h. Chloranil (2.20 mmol) was then added, and the mixture was stirred at reflux for 1 h. After evaporation of the solvent, the residue was purified by flash column chromatography.

General Method C: Preparation of Quaternary Ammonium Salts. The pyridyl- or quinolyl-substituted porphyrin free base (0.1 mmol) was dissolved in chloroform (5 mL) and diluted with 5 mL of nitromethane. The appropriate alkyl iodide (5 mmol) was added, and the mixture was heated at reflux under argon for 6 h and then evaporated to dryness. The residue was washed thoroughly with chloroform, taken up into 20 mL of water (or 3 mL of acetone and then diluted with 15 mL of water), and treated with 2 g of Dowex 1X2-200

anion-exchange resin in the chloride form, shaking slowly for 2 h. The resin was filtered off and washed with water, and the filtrate was lyophilized to give the chloride salt. The salt was further purified by chromatography on lipophilic Sephadex using methanol as the eluent.⁵³

5,10,15,20-Tetra(6-methyl-2-pyridyl)porphyrin (4). **4** was prepared by condensation of 6-methylpyridine-2-carboxaldehyde (0.78 g, 6.28 mmol) with pyrrole (0.454 mL, 6.28 mmol) in propionic acid (30 mL) according to general method A followed by chromatography (twice) on silica gel using chloroform–methanol (50:1 and then 20:1) as the eluent. The porphyrin **4** was isolated as a brown powder that recrystallized from dichloromethane–hexane (1:12) (0.13 g, 12%): ¹H NMR (CDCl₃) δ 8.82 (s, 8H), 7.99–7.90 (m, 8H), 7.53 (d, *J* = 7.0 Hz, 4H), 2.87 (s, 12H), –2.87 (s, 2H); MS (CI) *m/z* 675 (M + H).

5,15-Di(3-pyridyl)-10,20-di(3-quinolyl)porphyrin (5) and 5-(3-Pyridyl)-10,15,20-tri(3-quinolyl)porphyrin (6). Condensation of 3-pyridinecarboxaldehyde (1.07 g, 9.8 mmol), 3-quinolinecarboxaldehyde (1.57 g, 9.8 mmol), and pyrrole (1.39 mL, 19.6 mmol) in propionic acid (80 mL) according to general method A followed by chromatography (twice) using chloroform–methanol (8:1) and then chloroform–acetone (6:1) as the eluent gave **5** (176 mg, 5%) and **6** (75 mg, 2%). Data for **5**: ¹H NMR (CDCl₃) δ 9.83 (d, *J* = 1.7 Hz, 2H), 9.48 (s, 2H), 9.05 (dd, *J* = 1.5, 4.8 Hz, 2H), 9.00 (br s, 2H), 8.95–8.88 (m, 8H), 8.57 (d, *J* = 7.6 Hz, 2H), 8.49 (d, *J* = 8.4 Hz, 2H), 8.12 (d, *J* = 7.5 Hz, 2H), 7.98 (dt, *J* = 1.3, 7.0 Hz, 2H), 7.82–7.75 (m, 4H), –2.74 (br s, 2H); MS (CI) *m/z* 719 (M + H). Data for **6**: ¹H NMR (CDCl₃) δ 9.82 (d, *J* = 1.9 Hz, 3H), 9.45 (br s, 1H), 9.01 (br s, 4H), 8.93–8.86 (m, 8H), 8.56 (d, *J* = 7.8 Hz, 1H), 8.49 (d, *J* = 8.5 Hz, 3H), 8.13 (d, *J* = 7.8 Hz, 3H), 8.02–7.94 (m, 3H), 7.81–7.61 (m, 4H), –2.75 (br s, 2H); MS (CI) *m/z* 769 (M + H).

5-(4-Pyridyl)-10,15,20-tri(4-methylphenyl)porphyrin (7) and 5,15-Di(4-methylphenyl)-10,20-di(4-pyridyl)porphyrin. Condensation of 4-pyridinecarboxaldehyde (0.92 g, 8.42 mmol), 4-tolualdehyde (1.02 mL, 8.42 mmol), and pyrrole (1.17 mL, 16.8 mmol) in 60 mL of propionic acid according to general method A followed by chromatography on silica gel using dichloromethane–methanol (100:3) as the eluent gave **7** (4%) and 5,15-di(4-methylphenyl)-10,20-di(4-pyridyl)porphyrin, which was recrystallized from methanol–chloroform (4:1) as a purple solid (8%). Data for **7**: ¹H NMR (CDCl₃) δ 9.01 (d, *J* = 4.9 Hz, 2H), 8.92 (d, *J* = 4.8 Hz, 2H), 8.89 (s, 4H), 8.78 (d, *J* = 4.9 Hz, 2H), 8.16 (d, *J* = 5.7 Hz, 2H), 8.09 (d, *J* = 7.7 Hz, 6H), 7.53 (d, *J* = 7.7 Hz, 6H), 2.65 (s, 9H), –2.77 (s, 2H); MS (CI) *m/z* 657 (M + H). Data for 5,15-di(4-methylphenyl)-10,20-di(4-pyridyl)porphyrin: ¹H NMR (CDCl₃) δ 9.02 (d, *J* = 5.6 Hz, 6H), 8.93–8.89 (m, 6H), 8.79 (d, *J* = 5.0 Hz, 2H), 8.18 (d, *J* = 6.0 Hz, 6H), 8.09 (d, *J* = 7.8 Hz, 2H), 7.60 (d, *J* = 7.7 Hz, 2H), –2.90 (s, 2H); MS (CI) *m/z* 645 (M + 1).

5,15-Di(3-nitrophenyl)-10,20-di(4-pyridyl)porphyrin (8) and 5-(3-Nitrophenyl)-10,15,20-tri(4-pyridyl)porphyrin (9). Condensation of 4-pyridinecarboxaldehyde (1.26 mL, 12.9 mmol), 3-nitrobenzaldehyde (1.97 g, 12.9 mmol), and pyrrole (1.79 mL, 25.80 mmol) in 120 mL of propionic acid according to general method A followed by chromatography (twice) on silica gel eluting with chloroform–methanol (100:3) gave **8** (6%) and **9** (9%). Data for **8**: ¹H NMR (DMSO-*d*₆) δ 9.18 (d, *J* = 5.5 Hz, 4H), 9.00–8.85 (m, 4H), 8.90 (br s, 2H), 8.50 (br d, 4H), 8.41 (d, *J* = 7.5 Hz, 4H), 8.36 (s, 2H), 8.02 (m, 2H), 7.60 (s, 2H), –3.01 (s, 2H); MS (CI) *m/z* 707 (M + H). Data for **9**: ¹H NMR (CDCl₃) δ 9.05–8.96 (m, 8H), 8.84 (s, 6H), 8.78 (br d, 1H), 8.68 (d, *J* = 7.8 Hz, 1H), 8.48 (d, *J* = 7.9 Hz, 1H), 8.90 (d, *J* = 5.3 Hz, 6H), 7.96 (t, *J* = 7.5 Hz, 1H), –2.90 (s, 2H); MS (CI) *m/z* 663 (M + H).

5,15-Di(3-hydroxy-4-nitrophenyl)-10,20-di(4-pyridyl)porphyrin (10). Condensation of 4-pyridinecarboxaldehyde, 3-hydroxy-4-nitrobenzaldehyde, and pyrrole (1:1:2) in propionic acid according to general method A followed by chromatography on silica gel using chloroform–acetone (6:1) as the eluent gave **10** (6%): ¹H NMR (CDCl₃) δ 11.06 (s, 2H), 9.03 (d, *J* = 5.4 Hz, 4H), 8.89–8.82 (m, 8H), 8.47 (d, *J* = 8.6 Hz, 2H), 8.15

(d, *J* = 5.7 Hz, 4H), 8.00 (d, *J* = 1.8 Hz, 2H), 7.85–7.80 (m, 2H), –3.01 (s, 2H); MS (CI) *m/z* 739 (M + H), 721.

5-(3-Carboxyphenyl)-10,15,20-tri(4-pyridyl)porphyrin (11) and 5,15-Di(3-carboxyphenyl)-10,20-di(4-pyridyl)porphyrin (12). Condensation of 4-pyridinecarboxaldehyde (1.51 mL, 15.82 mmol), 3-carboxybenzaldehyde (2.38 g, 15.82 mmol), and pyrrole (2.4 mL, 34.59 mmol) in 150 mL of propionic acid according to general method A followed by chromatography (twice) on silica gel eluting with chloroform–methanol–acetic acid (110:10:1) gave **11** (7%) and **12** (4%). Data for **11**: ¹H NMR (DMSO-*d*₆) δ 13.01 (br s, 1H), 9.00 (br s, 6H), 8.86 (br s, 8H), 8.71 (br s, 1H), 8.46–8.41 (m, 2H), 8.23 (br s, 6H), 7.95 (br s, 1H), –2.98 (br s, 2H); MS (CI) *m/z* 662 (M + H). Data for **12**: ¹H NMR (DMSO-*d*₆) δ 12.80 (br s, 2H), 9.03 (d, *J* = 5.4 Hz, 4H), 8.89–8.82 (m, 8H), 8.70 (br s, 2H), 8.44–8.41 (m, 4H), 8.26 (br d, 4H), 8.00–7.94 (m, 2H), –3.00 (s, 2H); MS (CI) *m/z* 705 (M + H).

5-(4-Carboxyphenyl)-10,15,20-tri(4-pyridyl)porphyrin (13). **13** was prepared by condensation of 4-pyridinecarboxaldehyde (1.46 mL, 15 mmol), 4-carboxybenzaldehyde (0.77 g, 5 mmol), and pyrrole (1.49 mL, 21 mmol) in 15 mL of propionic acid according to general method A. Chromatography twice on silica eluting with chloroform–methanol (10:1 and then 95:6) gave **13** (0.13 g, 4%): ¹H NMR (DMSO-*d*₆) δ 13.21 (br s, 1H), 9.06 (d, *J* = 5.4 Hz, 6H), 8.84–8.80 (m, 8H), 8.36 (d, *J* = 8.2 Hz, 2H), 8.28 (d, *J* = 4.8 Hz, 6H), 8.20 (d, *J* = 8.1 Hz, 2H), –2.89 (br s, 2H); MS (CI) *m/z* 662 (M + H).

5,10,15,20-Tetra(4-chloro-3-nitrophenyl)porphyrin (14). **14** was prepared from 4-chloro-3-nitrobenzaldehyde and pyrrole (1:1) in propionic acid according to general method A. Chromatography on silica eluting with chloroform yielded **14** as a purple solid (25%): ¹H NMR (CF₃CO₂D) δ 9.23 (s, 4H), 8.49 (s, 8H), 8.71 (d, *J* = 8.2 Hz, 4H), 8.21 (dd, *J* = 1.2, 8.0 Hz, 4H); MS (CI) *m/z* 933 (M + H); HRMS (M + H) calcd 931.0393, found 931.0396, C₄₄H₂₃Cl₄N₈O₈.

5,10,15,20-Tetra(4-methoxy-3-hydroxyphenyl)porphyrin (15). **15** was prepared by condensation of pyrrole with 3-hydroxy-4-methoxybenzaldehyde (1:1) in propionic acid according to general method A. Chromatography on silica eluting with chloroform–methanol (25:1) gave **15** as a purple solid (36%): ¹H NMR (CDCl₃) δ 8.86 (s, 8H), 7.79 (d, *J* = 1.7 Hz, 4H), 7.63 (dd, *J* = 1.9, 8.2 Hz, 4H), 7.16 (d, *J* = 8.0 Hz, 4H), 5.88 (br s, 4H), 4.13 (s, 12H), –2.38 (s, 2H); MS (CI) *m/z* 799 (M + H); HRMS (M + H) calcd 799.2768, found 799.2772, C₄₈H₃₉N₄O₈.

5-(3-Aminophenyl)-10,15,20-tri(4-pyridyl)porphyrin (16). Stannous chloride dihydrate (0.98 g, 4.33 mmol) was added to a solution of the (nitrophenyl)porphyrin **9** (0.18 g, 0.272 mmol) in 6 M HCl (15 mL). The mixture was stirred at room temperature for 16 h, after which the solution was diluted with water (10 mL), neutralized with aqueous ammonia to pH 8, and extracted with chloroform (3 × 80 mL). The combined organic phase was washed with water, dried over anhydrous K₂CO₃, and evaporated to give **16** (0.124 g, 72%): ¹H NMR (CDCl₃) δ 9.04 (d, *J* = 5.9 Hz, 6H), 8.89 (d, *J* = 4.9 Hz, 2H), 8.85 (s, 4H), 8.80 (br s, 2H), 8.16 (br s, 6H), 7.99 (br s, 3H), 7.34 (s, 1H), –3.03 (s, 2H); MS (CI) *m/z* 633 (M + H).

5-(3-Acetylaminophenyl)-10,15,20-tri(4-pyridyl)porphyrin (17). A mixture of **16** (30 mg, 47 μmol), acetic anhydride (2 mL), and triethylamine (1 mL, 7.2 mmol) in 10 mL of dry chloroform was heated overnight. After evaporation of solvents and chromatography on silica eluting with chloroform–methanol–acetic acid (100:10:1), **17** was obtained as a solid (21 mg, 65%): ¹H NMR (CDCl₃) δ 9.02 (d, *J* = 5.8 Hz, 6H), 8.91 (d, *J* = 4.9 Hz, 2H), 8.82 (s, 4H), 8.79 (br d, 2H), 8.30 (br s, 1H), 8.17 (d, *J* = 6.2 Hz, 6H), 7.98 (br s, 1H), 7.69–7.65 (m, 2H), 6.82 (s, 1H), 2.23 (s, 3H), –3.03 (s, 2H); MS (CI) *m/z* 675 (M + H); HRMS (M + H) calcd 675.2621, found 675.2613, C₄₃H₃₁N₈O.

5-(3-Carboxamidophenyl)-10,15,20-tri(4-pyridyl)porphyrin (18). Carbonyldiimidazole (14 mg, 86 μmol) was added to a solution of porphyrin **11** (65 mg, 98 μmol) in 8 mL of dry THF, and the mixture was heated under reflux for 1 h under a nitrogen atmosphere. The reaction mixture was cooled to room temperature, concentrated aqueous ammonium hydrox-

ide was added (1 mL), and the mixture was stored at room temperature overnight.⁶² The porphyrin was extracted into chloroform (60 mL), washed with saturated aqueous NaHCO₃, and dried over Na₂SO₄. Chromatography on silica eluting with chloroform–methanol–acetic acid (100:10:1) gave **18** as a solid (58 mg, 89%): ¹H NMR (CDCl₃) δ 9.03 (d, *J* = 6.8 Hz, 6H), 8.9 (m, 8H), 8.70 (br s, 1H), 8.46 (m, 2H), 8.28 (d, *J* = 6.8 Hz, 6H), 7.94 (br s, 1H), 7.55 (s, 2H), –2.81 (s, 2H); MS (CI) *m/z* 661 (M + H); HRMS (M + H) calcd 661.2464, found 661.2430, C₄₂H₂₉N₈O.

5,15-Di(3-carboxamidophenyl)-10,20-di(4-pyridyl)porphyrin (19). **19** was prepared from **12** by a method similar to the preparation of **18** in 55% yield: ¹H NMR (DMSO-*d*₆) δ 9.16 (d, *J* = 5.5 Hz, 4H), 8.96–8.86 (m, 6H), 8.71 (br s, 2H), 8.49 (br d, 4H), 8.38 (d, *J* = 7.7 Hz, 4H), 8.26 (br s, 2H), 7.93 (t, *J* = 7.6 Hz, 2H), 7.58 (br s, 2H), –2.98 (s, 2H); MS (CI) *m/z* 703 (M + H), 686; HRMS (M + H) calcd 703.2570, found 703.2566, C₄₄H₃₁N₈O₂.

5-Bromo-3-(hydroxymethyl)pyridine (20). To a solution of 5-bromonicotinic acid (6.1 g) in 80 mL of distilled THF under argon was added 60 mL of 1.0 M borane–tetrahydrofuran complex, and the mixture was stirred at reflux under argon for 4 h. HCl (1 M) was added, and the mixture was adjusted to pH 8 with 2 M NaOH and then extracted with EtOAc (5 × 100 mL). The combined organic phase was carefully washed with water and dried over K₂CO₃. After removal of solvent, the residue was chromatographed using EtOAc as the eluent to give **20** as a colorless oil (1.65 g, 29%): ¹H NMR (CDCl₃) δ 8.34 (d, *J* = 2.1 Hz, 1H), 8.26 (d, *J* = 1.6 Hz, 1H), 7.77 (t, *J* = 1.9 Hz, 1H), 5.26 (br s, 1H), 4.57 (s, 2H); MS (CI) *m/z* 189 (M + 1).

3-(Hydroxymethyl)-5-(2-thiophene)pyridine (21). To a mixture of **20** (0.36 g, 1.91 mmol), thiophene-3-boronic acid (0.25 g, 1.91 mmol), and Pd(PPh₃)₄ (22 mg, 19.2 μmol) were added 10 mL of toluene and 2.5 mL of methanol under argon, followed by 4 mL of 2 M aqueous Na₂CO₃. The reaction mixture was stirred at 70 °C under argon for 20 h. After removal of solvent, the residue was chromatographed using EtOAc–hexane (14:5) and EtOAc as the eluent to give **21** as a purple oil (0.24 g, 65%): ¹H NMR (CDCl₃) δ 8.69 (d, *J* = 2.0 Hz, 1H), 8.39 (d, *J* = 1.9 Hz, 1H), 7.89 (t, *J* = 2.1 Hz, 1H), 7.34 (q, *J* = 1.2, 2.5 Hz, 1H), 7.32 (s, 1H), 7.08 (q, *J* = 3.9, 4.8, 1H), 4.74 (s, 2H), 3.71 (br s, OH); MS (CI) *m/z* 192 (M + 1).

3-(Hydroxymethyl)-5-(3-thiophene)pyridine (22). **22** was prepared from **20** (0.36 g, 1.91 mmol), thiophene-2-boronic acid (0.25 g, 1.91 mmol), Pd(PPh₃)₄ (22 mg) in 10 mL of toluene, 2.5 mL of MeOH, and 4 mL of 2 M aqueous Na₂CO₃ according to the procedure of **21** as a brown-yellow oil (0.223 g, 61%): ¹H NMR (CDCl₃) δ 8.74 (d, *J* = 2.2 Hz, 1H), 8.45 (d, *J* = 2.1 Hz, 1H), 7.91 (t, *J* = 2.1 Hz, 1H), 7.52 (q, *J* = 1.4, 2.9 Hz, 1H), 7.42 (d, *J* = 2.9 Hz, 1H), 7.38 (q, *J* = 1.4, 5.1 Hz, 1H), 4.77 (s, 2H), 2.80 (br s, OH); MS (CI) *m/z* 192 (M + 1).

3-Formyl-5-(2-thiophene)pyridine (23) and 5,10,15,20-Tetra[5-(2-thiophene)-3-pyridyl]porphyrin (26). To a stirred suspension of pyridinium chlorochromate (0.37 g, 1.74 mmol) and sodium acetate (32 mg) in 8 mL of dichloromethane under argon was added a solution of **21** (0.22 g, 1.15 mmol) in 8 mL of dichloromethane. The reaction mixture was stirred at room temperature under argon for 2 h and then poured into 100 mL of ether. This was filtered through a funnel that had a layer of silica gel at the bottom with Celite on top, and washed with EtOAc–hexanes (3:2). The filtrate was monitored by TLC. After removal of solvent, an oil was obtained (0.104 g, 48%): MS (CI) *m/z* 190 (M + 1). TLC (EtOAc) showed only one spot. This crude aldehyde **23** was not purified further. Preparation of porphyrin **26** was by condensation of aldehyde **23** with pyrrole (1:1) in propionic acid according to general method A: MS (CI) *m/z* 947 (M + 1); HRMS (M + H) calcd 947.1868, found 947.1872, C₅₆H₃₅N₈S₄.

3-Formyl-5-(3-thiophene)pyridine (24). Treatment of **22** (0.20 g, 1.04 mmol) with PCC (0.33 g, 1.56 mmol) and sodium acetate (30 mg) according to the procedure of **23** gave **24** as an oil (0.10 g, 52%): MS (CI) *m/z* 190 (M + 1). TLC (EtOAc)

showed only one spot. This crude product was used directly in the preparation of porphyrins.

5-Bromo-3-formylpyridine (25). Treatment of **20** (1.07 g, 5.68 mmol) with PCC (1.88 g, 8.52 mmol) and sodium acetate (150 mg) according to the procedure of **23** gave **25** as white crystals (0.43 g, 40%): mp 37–39 °C; ¹H NMR (CDCl₃) δ 10.03 (s, 1H), 8.93 (d, *J* = 1.9 Hz, 1H), 8.85 (d, *J* = 1.6 Hz, 1H), 8.24 (d, *J* = 1.5 Hz, 1H); MS (CI) *m/z* 187 (M + 1).

5,10,15,20-Tetra[5-bromo-3-pyridyl]porphyrin (27). Condensation of **25** (1.51 g, 8.12 mmol) with pyrrole (0.79 mL, 11.39 mmol) in propionic acid according to general method A followed by chromatography on silica gel with chloroform–acetone (6:1) yielded **27** (0.35 g 18%): ¹H NMR (CDCl₃) δ 9.34 (br s, 4H), 9.14 (d, *J* = 2.2 Hz, 4H), 8.86 (br s, 8H), 8.65 (br s, 4H), –2.94 (s, 2H); MS (CI) *m/z* 935 (M + 1). Anal. Calcd for C₄₀H₂₂Br₄N₈: C, 51.42; H, 2.37; N, 11.99. Found: C, 51.53; H, 2.40; N, 11.96.

5,10,15,20-Tetra[5-(2-furfuryl)-3-pyridyl]porphyrin (28). To a mixture of compound **27** (61 mg, 65 μmol), 2-furanboronic acid (60 mg, 520 μmol), and Pd(PPh₃)₄ (2 mg, 1.74 μmol) in a mixture of toluene (7.5 mL) and methanol (1.8 mL) under argon was added 2 M aqueous sodium carbonate (1.5 mL) via a syringe. The reaction mixture was stirred at 70 °C for 20 h. Further boronic acid (25 mg) and Pd(PPh₃)₄ (1 mg) were added, and the reaction continued for another 15 h. The mixture was poured into 40 mL of water and extracted with chloroform (3 × 60 mL). The combined extracts were dried over anhydrous Na₂SO₄, filtered, and evaporated. The product was purified by flash chromatography eluting with chloroform–acetone (5:1) to give **28** as a brown solid (25 mg, 44%): ¹H NMR (CDCl₃) δ 9.35 (d, *J* = 2 Hz, 4H), 9.29 (br s, 4H), 8.91 (br s, 8H), 8.76 (br s, 4H), 7.56 (s, 4H), 6.96 (d, *J* = 3.2 Hz, 4H), 6.56 (m, 4H), –2.82 (s, 2H); MS (CI) *m/z* 883 (M + 1); HRMS (M + H) calcd 883.2781, found 883.2785, C₅₆H₃₅N₈O₄. Anal. Calcd for C₅₆H₃₄N₈O₄: C, 76.18; H, 3.88; N, 12.69. Found: C, 76.16; H, 3.85; N, 12.71.

5,10,15,20-Tetra[5-(3-thiophene)-3-pyridyl]porphyrin (29) and 5-(5-Bromo-3-pyridyl)-10,15,20-tri[5-(3-thiophene)-3-pyridyl]porphyrin (30). **29** and **30** were prepared from compound **27** (30 mg, 32 μmol), 3-thiopheneboronic acid (36 mg, 281 μmol), and Pd(PPh₃)₄ (1 mg) according to the procedure for the preparation of **28**. Flash chromatography was used, eluting with chloroform–acetone (5:1), to give **29** (4 mg, 13%) and **30** (10.5 mg, 35%). Data for **29**: ¹H NMR (CDCl₃) δ 9.36 (br, 4H), 9.31 (s, 4H), 8.94 (br s, 8H), 8.72 (br s, 4H), 7.76 (br s, 4H), 7.09 (d, *J* = 4.5 Hz, 4H), 7.51 (br d, 4H), –2.80 (s, 2H); HRMS (M + H) calcd 947.1868, found 947.1842, C₅₆H₃₅N₈S₄. Data for **30** (10.5 mg, 35%): ¹H NMR (CDCl₃) δ 9.45 (br, 3H), 9.32 (br, 1H), 9.27 (br, 3H), 9.40 (br, 1H), 8.92 (br, 4H), 8.87 (br, 3H), 8.68 (s, 4H), 8.65 (br, 1H), 7.78 (br, 3H), 7.71 (br, 3H), 7.65 (d, *J* = 3.6 Hz, 3H), –2.74 (s, 1H), –2.26 (s, 2H); MS (CI) *m/z* 943 (M + 1); HRMS (M + H) calcd 943.1095, found 943.1089, C₅₂H₃₂BrN₈S₃.

2,2'-Dipyrrylmethane (31). To a solution of thiophosgene (2.79 mL, 35.4 mmol) in 100 mL of benzene at 0 °C was added dropwise a solution of a pyrrole (5.28 mL, 73 mmol) in 50 mL of anhydrous ether. The resulting mixture was stirred at 0 °C for 10 min, and then 120 mL of aqueous methanol (80%) was added. The mixture was stirred for 45 min at room temperature. Evaporation of solvent gave the crude 2,2'-dipyrryl thioketone: MS (CI) *m/z* 177 (M + 1). The crude 2,2'-dipyrryl thioketone was dissolved in 350 mL of 95% ethanol containing 9 g of KOH. To this solution was added 90 mL of 5% aqueous H₂O₂. The mixture was immediately heated on a steam bath for 5 min and then poured into 800 mL of water. The solution was extracted with CHCl₃ until no product remained in the aqueous solution. The combined organic phase was washed carefully with water, dried over K₂CO₃, and evaporated to afford yellow crystals of 2,2'-dipyrryl ketone (4.46 g, 76%): mp 157–159 °C (lit.⁵² mp 158–159 °C); ¹H NMR (CDCl₃) δ 10.01 (br s, 2H), 7.08 (dt, *J* = 1.3, 2.7 Hz, 2H), 6.33 (dt, *J* = 2.5, 3.8 Hz, 2H); MS (CI) *m/z* 161 (M + 1).

2,2'-Dipyrryl ketone (1 g) was reduced by NaBH₄ in the presence of morpholine according to the literature procedure

to give **31** as pale yellow crystals (0.78 g, 85%): mp 72–73 °C (lit.⁵² mp 73 °C); ¹H NMR (CDCl₃) δ 7.85 (br s, 2H), 6.65 (dt, *J* = 1.6, 2.7 Hz, 2H), 6.14 (dd, *J* = 2.8, 5.8 Hz, 2H), 6.04–6.01 (m, 2H), 3.97 (s, 2H); MS (CI) *m/z* 147 (*M* + 1).

5,15-Di(4-hydroxy-3-nitrophenyl)porphyrin (32). Treatment of **31** and 3-nitro-4-hydroxybenzaldehyde according to general method B gave **32** as a pale purple solid in 69% yield: ¹H NMR (DMSO-*d*₆) δ 11.60 (s, 2H), 10.67 (s, 2H), 9.69 (d, *J* = 4.5 Hz, 4H), 9.14 (d, *J* = 4.5 Hz, 4H), 8.73 (br s, 2H), 8.43 (d, *J* = 8.5 Hz, 2H), 7.62 (d, *J* = 8.6 Hz, 2H), –3.24 (s, 2H); MS (CI) *m/z* 585 (*M* + 1), 567, 249; HRMS (*M* + H) calcd 585.1523, found 585.1220, C₃₂H₂₁N₆O₆. Anal. Calcd for C₃₂H₂₀N₆O₆: C, 65.75; H, 3.45; N, 14.38. Found: C, 65.72; H, 3.48; N, 14.41.

5,15-Di(3-hydroxy-4-nitrophenyl)porphyrin (33). Treatment of **31** and 4-nitro-3-hydroxybenzaldehyde according to general method B gave **33** as a pale purple solid in 65% yield: ¹H NMR (DMSO-*d*₆) δ 11.53 (s, 2H), 10.71 (s, 2H), 9.71 (t, *J* = 4.6 Hz, 4H), 9.17 (d, *J* = 4.5 Hz, 4H), 8.37 (d, *J* = 8.6 Hz, 2H), 8.01 (s, 2H), 7.89 (d, *J* = 8.4 Hz, 2H), –3.34 (s, 2H); MS (CI) *m/z* 585 (*M* + 1); HRMS (*M* + H) calcd 585.1523, found 585.1519, C₃₂H₂₁N₆O₆. Anal. Calcd for C₃₂H₂₀N₆O₆: C, 65.75; H, 3.45; N, 14.38. Found: C, 65.79; H, 3.42; N, 14.35.

5,15-Di(3-nitrophenyl)porphyrin (34). Treatment of **31** and 3-nitrobenzaldehyde according to general method B gave **34** as a purple solid in 74% yield: ¹H NMR (CDCl₃) δ 10.46 (s, 2H), 9.47 (br s, 4H), 9.16 (s, 2H), 8.89 (br s, 4H), 8.69 (br t, 2H), 8.56 (br d, 2H), 8.08–7.92 (m, 4H), –3.50 (s, 2H); MS (CI) *m/z* 553 (*M* + 1); HRMS (*M* + H) calcd 553.1624, found 553.1619, C₃₂H₂₁N₆O₄. Anal. Calcd for C₃₂H₂₀N₆O₄: C, 69.56; H, 3.65; N, 15.21. Found: C, 69.60; H, 3.68; N, 15.25.

5,15-Di(3-hydroxy-4-methoxyphenyl)porphyrin (35). Treatment of **31** and 4-methoxy-3-hydroxybenzaldehyde according to general method B gave **35** as a brown solid in 82% yield: ¹H NMR (DMSO-*d*₆) δ 10.58 (s, 2H), 9.61 (d, *J* = 4.6 Hz, 4H), 9.53 (s, 2H), 9.10 (d, *J* = 4.6 Hz, 4H), 7.71 (d, *J* = 1.6 Hz, 2H), 7.63 (d, *J* = 8.0 Hz, 2H), 7.39 (d, *J* = 8.4 Hz, 2H), –3.25 (s, 2H); MS (CI) *m/z* 555 (*M* + H), 540; HRMS (*M* + H) calcd 555.2032, found 555.2039, C₃₄H₂₇N₄O₄. Anal. Calcd for C₃₄H₂₆N₄O₄: C, 73.63; H, 4.73; N, 10.10. Found: C, 73.60; H, 4.76; N, 10.12.

5,10,15,20-Tetra(6-methyl-*N*-methyl-2-pyridyl)porphyrin Chloride (36). **36** was prepared from **4** and iodomethane according to general method C in 89% yield: ¹H NMR (D₂O) δ 9.41–7.52 (m, 20H), 3.81 (s, 12H), 2.73 (s, 12H); HRMS (FAB) (*M*) calcd 734.3845, found 734.3840, C₄₈H₄₆N₈.

5,15-Di(*N*-methyl-3-pyridyl)-10,20-di(*N*-methyl-3-quinoly)porphyrin Chloride (37). **37** was prepared from **5** and iodomethane according to general method C in 92% yield: ¹H NMR (D₂O) δ 10.06–7.84 (m, 26H), 4.59 (s, 9H), 4.49 (s, 3H); HRMS (FAB) (*M*) calcd 778.3532, found 778.3529, C₅₂H₄₂N₈.

5-(*N*-Methyl-3-pyridyl)-5,10,15-tri(*N*-methyl-3-quinoly)porphyrin Chloride (38). **38** was prepared from **6** and iodomethane according to general method C in 89% yield: ¹H NMR (D₂O) δ 10.03–7.76 (m, 30H), 4.50 (s, 3H), 4.33 (s, 9H); HRMS (FAB) (*M*) calcd 828.3689, found 828.3693, C₅₆H₄₄N₈.

5-(*N*-Methyl-4-pyridyl)-10,15,20-tri(4-methylphenyl)porphyrin Chloride (39). **39** was prepared from **7** and iodomethane according to general method C, with ion exchange in acetone–water (10:1), in 69% yield: ¹H NMR (DMSO-*d*₆) δ 9.43 (br d, 2H), 8.96–8.86 (m, 10H), 8.09 (br d, 6H), 7.65 (br d, 6H), 4.67 (s, 3H), 2.49 (s, 9H); MS (FAB) 673 (*M*); HRMS (FAB) (*M*) calcd 672.3127, found 672.3124, C₄₇H₃₈N₅.

5,15-Di(*N*-methyl-4-pyridyl)-10,20-di(3-nitrophenyl)porphyrin Chloride (40). **40** was prepared from **8** according to general method C in 79% yield: ¹H NMR (D₂O) δ 9.61–7.21 (m, 24H), 4.60 (s, 6H); HRMS (FAB) (*M*) calcd 736.2547, found 736.2541, C₄₄H₃₂N₈O₄.

5-(3-Nitrophenyl)-10,15,20-tri(*N*-methyl-4-pyridyl)porphyrin Chloride (41). **41** was prepared from **9** and iodomethane according to general method C in 79% yield: ¹H NMR (D₂O) δ 9.51–7.18 (m, 24H), 4.62 (s, 9H); HRMS (*M*) calcd 707.2883, found 707.2872, C₄₄H₃₅N₈O₂.

5-(3-Carboxyphenyl)-10,15,20-tri(*N*-methyl-4-pyridyl)porphyrin Chloride (42). **42** was prepared from **11** and iodomethane according to general method C in 76% yield: ¹H NMR (D₂O) δ 9.02–8.10 (m, 20H), 7.96 (s, 1H), 7.26–7.21 (m, 3H), 4.56 (s, 9H); HRMS (FAB) (*M*) calcd 706.2930, found 706.2917, C₄₅H₃₆N₇O₂.

5,15-Di(3-carboxyphenyl)-10,20-di(*N*-methyl-4-pyridyl)porphyrin Chloride (43). **43** was prepared from **12** and iodomethane according to general method C in 79% yield: ¹H NMR (D₂O) δ 9.05–7.90 (m, 24H), 4.55 (s, 6H); HRMS (FAB) (*M*) calcd 734.2642, found 734.2653, C₄₆H₃₄N₆O₄.

5,15-Di[3-(2-bromoethylcarboxamido)phenyl]-10,20-di(*N*-methyl-4-pyridyl)porphyrin Chloride (44). A solution of the diacid **12** (76 mg, 0.11 mmol) and carbonyldiimidazole (46 mg, 0.26 mmol) in dry THF was stirred under reflux in an argon atmosphere for 1.5 h. After the solution was cooled to room temperature, 2-bromoethylamine hydrobromide (0.115 g, 0.5 mmol) was added followed by 0.1 mL of triethylamine, and the mixture was stirred at room temperature for 24 h. After evaporation of the solvent, the residue was dissolved in 20 mL of chloroform and then washed with 10% sodium carbonate (10 mL) and water (twice 20 mL). The porphyrin free base was purified by preparative TLC developed with CHCl₃–MeOH (3:1): MS (CI) 917 (*M* + 1), 915. The product was then alkylated with iodomethane according to general procedure C to give **44** (49 mg, 45%): HRMS (FAB) (*M*) calcd 944.1798, found 944.1792, C₅₀H₄₂Br₂N₈O₂. Anal. Calcd for C₅₀H₄₂Br₂Cl₂N₈O₂: C, 59.01; H, 4.16; N, 11.01. Found: C, 59.05; H, 4.12; N, 11.06.

5-(4-Carboxyphenyl)-10,15,20-tri(*N*-methyl-4-pyridyl)porphyrin Chloride (45). **45** was prepared from **13** and iodomethane according to general method C in 80% yield: ¹H NMR (D₂O) δ 9.10–8.06 (m, 24H), 4.60 (s, 9H); HRMS (FAB) (*M*) calcd 706.2930, found 706.2915, C₄₅H₃₆N₇O₂.

5-(3-Acetylaminophenyl)-10,15,20-tri(*N*-methyl-4-pyridyl)porphyrin Chloride (46). **46** was prepared from **17** and iodomethane according to general method C in 58% yield: ¹H NMR (D₂O) δ 9.12–8.36 (m, 20H), 7.86–7.66 (m, 4H), 4.54 (s, 9H), 3.29 (s, 3H); HRMS (*M*) calcd 719.3247, found 719.3234, C₄₆H₃₈N₈O.

5-(3-Carboxamidophenyl)-10,15,20-tri(*N*-methyl-4-pyridyl)porphyrin Chloride (47). **47** was prepared from **18** with iodomethane according to general method C in 66% yield: ¹H NMR (D₂O) δ 9.01–8.25 (m, 20H), 8.03–7.39 (m, 4H), 4.61 (s, 9H); HRMS (FAB) (*M*) calcd 705.3090, found 705.3079, C₄₅H₃₇N₈O.

5,15-Di(3-carboxamidophenyl)-15,20-di(*N*-methyl-4-pyridyl)porphyrin Chloride (48). **48** was prepared from **19** with iodomethane according to general method C in 88% yield: ¹H NMR (D₂O) δ 9.48–8.67 (m, 16H), 7.85 (s, 2H), 7.73–7.20 (m, 6H), 4.61 (s, 6H); HRMS (FAB) (*M*) calcd 732.2961, found 732.2971, C₄₆H₃₆N₈O₂.

5,10,15,20-Tetra(*N*-ethyl-4-pyridyl)porphyrin Chloride (49). **49** was prepared from 5,10,15,20-tetra(4-pyridyl)porphyrin with iodomethane according to general method C in 96% yield: ¹H NMR (D₂O) δ 9.13–8.01 (m, 24H), 4.90–4.87 (m, 8H), 1.81–1.75 (m, 12H); HRMS (FAB) (*M*) calcd 734.3845, found 734.3850, C₄₈H₄₆N₈.

5,10,15,20-Tetra[*N*-(acetoxymethyl)-4-pyridyl]porphyrin Chloride (50). **50** was prepared from 5,10,15,20-tetra(4-pyridyl)porphyrin with bromomethyl acetate according to general method C in 91% yield: ¹H NMR (D₂O) δ 9.51 (d, *J* = 6.2 Hz, 8H), 9.24–8.97 (m, 16H), 6.75 (s, 8H), 2.31 (s, 12H); HRMS (FAB) (*M*) calcd 910.3439, found 910.3442, C₅₂H₄₆N₈O₈.

5,10,15,20-Tetra[5-(2-furfuryl)-*N*-methyl-3-pyridyl]porphyrin Chloride (57). **57** was prepared from **28** with iodomethane according to general method C in 61% yield: ¹H NMR (D₂O) δ 9.42–8.94 (m, 20H), 7.55–6.56 (m, 12H), 4.54 (s, 12H); HRMS (FAB) (*M*) calcd 942.3642, found 942.3649, C₆₀H₄₆N₈O₄. Anal. Calcd for C₆₀H₄₆Cl₂N₈O₄·2H₂O: C, 64.29; H, 4.50; N, 10.00. Found: C, 64.32; H, 4.48; N, 9.98.

Telomerase Assay. Telomerase assays were run as previously described.^{24,54} All reactions were carried out in amber Eppendorf tubes under subdued lighting to avoid photocleav-

age. Briefly, reaction mixtures (20 μ L) contained 4 μ L of cell extracts (60 μ g of total cell protein), 50 mM Tris-OAc (pH 8.5), 50 mM K-OAc, 1 mM $MgCl_2$, 5 mM BME, 1 mM spermidine, 1 μ M 5'-biotinylated telomere primer (TTAGGG)₃, 1.2 μ M [α -³²P]dGTP (800 Ci/mmol), 1 mM dATP, and 1 mM dTTP and were incubated at 37 °C for 30 min. Reactions were terminated by adding 20 μ L of Streptavidin-Dynabeads. Streptavidin-Dynabeads bind selectively to the desired targets (5'-biotinylated primer), forming a magnetic bead-target complex. This complex was separated from the suspension using a magnet (DynaL MPC) and washed several times with washing buffer (2 M NaCl) to eliminate the [α -³²P]dGTP background. Telomerase reaction products were separated from the magnetic beads by protein denaturation with 5.0 M guanidine-HCl at 90 °C for 30 min. After recovery of these products, analysis was performed by 8% denaturing PAGE. Telomerase activities were quantified by densitometric analyses of an autoradiogram using ImageQuaNT software (Molecular Dynamics). The results given in Tables 1–7 are from a single experiment. Our experience is that these numbers do fluctuate from one experiment to the next; however, the fluctuation within the same experiment is \pm 10%.

Acknowledgment. This work was supported by a grant from the National Institutes of Health (CA49751) and a National Cooperative Drug Discovery Group (NCDDG) grant (CA67760) from the National Cancer Institute. We thank Professor Daniel D. Von Hoff for his enthusiastic leadership of the NCDDG and other members of the telomerase group in Austin and San Antonio. We particularly thank Alvin Carter of Mid-century for many helpful discussions. Finally, we are grateful to Dr. David Bishop for proofreading, editing, and preparing the final version of the manuscript, tables, figures, and schemes.

Supporting Information Available: Synthetic details for a further three compounds and telomerase inhibition data for sixty-four compounds in six tables. This material is available free of charge via the Internet at <http://pubs.acs.org>.

References

- Han, H.; Hurley, L. H. G-quadruplex DNA: a potential target in anticancer drug design. *Trends Pharmacol. Sci.* **2000**, *21*, 136–142.
- Hurley, L. H.; Wheelhouse, R. T.; Sun, D.; Kerwin, S. M.; Salazar, M.; Fedoroff, O. Y.; Han, F. X.; Han, H.; Izbicka, E.; Von Hoff, D. D. G-quadruplexes as targets for drug design. *Pharmacol. Ther.* **2000**, *85*, 141–158.
- Kerwin, S. M. G-quadruplex DNA as a target for drug design. *Curr. Pharm. Des.* **2000**, *6*, 441–471.
- Jenkins, T. C. Targeting multi-stranded DNA structures. *Curr. Med. Chem.* **2000**, *7*, 99–115.
- Mergny, J.-L.; Hélène, C. G-quadruplex DNA: a target for drug design. *Nat. Med.* **1998**, *4*, 1366–1367.
- Raymond, E.; Sun, D.; Chen, S.-F.; Windle, B.; Von Hoff, D. D. Agents that target telomerase and telomeres. *Curr. Opin. Biotechnol.* **1996**, *7*, 583–591.
- Kelland, L. R. Telomerase: biology and phase 1 trials. *Lancet* **2001**, *2*, 95–102.
- Bearss, D. J.; Hurley, L. H.; Von Hoff, D. D. Telomere maintenance mechanisms as a target for drug development. *Oncogene* **2000**, *19*, 6632–6641.
- Simonsson, T.; Pecinka, P.; Kubista, M. DNA tetraplex formation in the control region of c-myc. *Nucleic Acids Res.* **1998**, *26*, 1167–1172.
- Castasi, P.; Chen, X.; Moyzis, R.; Bradbury, E.; Gupta, G. Structure-function correlations in the insulin-linked polymorphic region. *J. Mol. Biol.* **1996**, *264*, 534–545.
- Usdin, K.; Woodford, K. J. CGG Repeats associated with DNA instability and chromosome fragility form structures that block DNA synthesis *in vitro*. *Nucleic Acids Res.* **1995**, *23*, 4202–4209.
- Smith, S. S.; Laayoun, A.; Lingeman, R. G.; Baker, D. J.; Ridley, J. Hypermethylation of telomere-like foldbacks at codon-12 of the human C-HA-RAS gene and the trinucleotide repeat of the FMR-1 gene of fragile X. *J. Mol. Biol.* **1994**, *243*, 143–150.
- Freudenreich, C. H.; Kantrow, S. M.; Zakian, V. A. Expansion and length-dependent fragility of CTG repeats in yeast. *Science* **1998**, *279*, 853–856.
- Oliver, A. W.; Bogdarina, I.; Kneale, G. G. Preferential binding of Fd gene 5 protein to tetraplex nucleic acid structures. *J. Mol. Biol.* **2000**, *301*, 575–584.
- Harrington, C.; Lan, Y.; Akman, S. A. The identification and characterization of G4-DNA resolvase activity. *J. Biol. Chem.* **1997**, *272*, 24631–24636.
- Fang, G. W.; Cech, T. R. The β -subunit of *Oxytricha* telomere-binding protein promotes G-quartet formation by telomeric DNA. *Cell* **1993**, *74*, 875–885.
- Gilson, E.; Roberge, M.; Giraldo, R.; Rhodes, D.; Glasser, S. M. Distortion of the DNA double helix by RAP1 at silencers and multiple telomeric binding-sites. *J. Mol. Biol.* **1993**, *231*, 293–310.
- Kim, N. W.; Piatyszek, A. M.; Prowse, K. R.; Harley, C. B.; West, M. D.; Ho, P. L. C.; Coviello, G. M.; Wright, W. E.; Weinrich, S. L.; Shay, J. W. Specific association of human telomerase activity with immortal cells and cancer. *Science* **1994**, *266*, 2011–2015.
- Hahn, W. C.; Stewart, S. A.; Brooks, M. W.; York, S. G.; Eaton, E.; Kurachi, A.; Beijersbergen, R. L.; Knoll, J. H. M.; Meyerson, M.; Weinberg, R. A. Inhibition of telomerase limits the growth of human cancer cells. *Nat. Med.* **1999**, *5*, 1164–1170.
- de Lange, T.; Jacks, T. For Better or Worse? Telomerase inhibition and cancer. *Cell* **1999**, *96*, 273–275.
- Olovnikov, A. M. A theory of marginotomy. *J. Theor. Biol.* **1973**, *41*, 181–190.
- Makarov, V. L.; Hirose, Y.; Langmore, J. P. Long G-tails at both ends of human chromosomes suggest a C-strand degradation mechanism for telomere shortening. *Cell* **1997**, *88*, 657–666.
- Zahler, A. M.; Williamson, J. R.; Cech, T. R.; Prescott, D. M. Inhibition of telomerase by G-quartet structures. *Nature* **1991**, *350*, 718–720.
- Sun, D.; Thompson, B.; Cathers, B. E.; Salazar, M.; Kerwin, S. M.; Trent, J. O.; Jenkins, T. C.; Neidle, S.; Hurley, L. H. Inhibition of human telomerase by a G-quadruplex-interactive compound. *J. Med. Chem.* **1997**, *40*, 2113–2116.
- Wheelhouse, R. T.; Sun, D.; Han, H.; Han, F. X.; Hurley, L. H. Cationic porphyrins as telomerase inhibitors: the interaction of tetra(*N*-methyl-4-pyridyl)porphine with quadruplex DNA. *J. Am. Chem. Soc.* **1998**, *120*, 3261–3262.
- Perry, P. J.; Jenkins, T. C. Recent advances in the development of telomerase inhibitors for the treatment of cancer. *Exp. Opin. Invest. Drugs* **1999**, *8*, 1981–2008.
- Izbicka, E.; Wheelhouse, R. T.; Raymond, E.; Davidson, K. L.; Lawrence, R. A.; Sun, D.; Windle, B. E.; Hurley, L. H.; Von Hoff, D. D. Effects of cationic porphyrins as G-quadruplex interactive agents in human tumor cells. *Cancer Res.* **1999**, *59*, 639–644.
- Chen, Q.; Kuntz, I.; Shafer, R. Spectroscopic recognition of guanine dimeric hairpin quadruplexes by a carbocyanine dye. *Proc. Natl. Acad. Sci. U.S.A.* **1996**, *93*, 2635–2639.
- Perry, P. J.; Read, M. A.; Davies, R. T.; Gowan, S. M.; Reszka, A. P.; Wood, A. A.; Kelland, L. R.; Neidle, S. 2,7-Disubstituted amidofluorenone derivatives as inhibitors of human telomerase. *J. Med. Chem.* **1999**, *42*, 2679–2684.
- Perry, P. J.; Gowan, S. M.; Read, M. A.; Kelland, L. R.; Neidle, S. Design, synthesis and evaluation of human telomerase inhibitors based upon a tetracyclic structural motif. *Anti-Cancer Drug Des.* **1999**, *14*, 373–382.
- Fedoroff, O. Y.; Salazar, M.; Han, H.; Chemeris, V. V.; Kerwin, S. M.; Hurley, L. H. NMR-based model of a telomerase-inhibiting compound bound to G-quadruplex DNA. *Biochemistry* **1998**, *37*, 12367–12374.
- Guo, Q.; Lu, M.; Marky, L. A.; Kallenbach, N. R. Interaction of the dye ethidium bromide with DNA containing guanine repeats. *Biochemistry* **1992**, *31*, 2451–2455.
- Koeppel, F.; Riou, J.-F.; Laoui, A.; Malliet, P.; Arimondo, P. B.; Labit, D.; Petigenet, O.; Hélène, C.; Mergny, J.-L. Ethidium derivatives bind to G-quartets, inhibit telomerase, and act as fluorescent probes for quadruplexes. *Nucleic Acids Res.* **2001**, *29*, 1087–1096.
- Gowan, S. M.; Brunton, L.; Valenti, M.; Heald, R.; Read, M. A.; Harrison, J. R.; Stevens, M. F. G.; Neidle, S.; Kelland, L. R. Preclinical antitumor properties of G-quadruplex-interactive small molecule inhibitors of telomerase. *Proc. Am. Assoc. Cancer Res.* **2001**, *42*, abstract 466.
- Riou, J.-F.; Mailliet, P.; Laoui, A.; Renou, E.; Petigenet, O.; Guittat, L.; Mergny, J.-L. Apoptosis, cell senescence, and telomere shortening induced by a new series of specific G-quadruplex DNA ligand. *Proc. Am. Assoc. Cancer Res.* **2001**, *42*, abstract 4496.
- Wheelhouse, R. T.; Hurley, L. H. Porphyrin Compounds as Telomerase Inhibitors. International Publication WO 98/33503, 1998.
- Shammas, M. A.; Batchu, R. B.; Wang, J. Y.; Hurley, L. H.; Shmookler Reis, R. J.; and Munshi, N. C. Telomerase inhibition and cell growth arrest following porphyrin treatment of multiple myeloma cells. *Gene*, submitted for publication.

- (38) Lipscomb, L. A.; Zhou, F. X.; Presnell, S. R.; Woo, R. J.; Peek, M. E.; Plakston, R. R.; Williams, L. D. Structure of a DNA-porphyrin complex. *Biochemistry* **1996**, *35*, 2818–2823.
- (39) Guliaev, A. B.; Leontis, N. B. Cationic 5,10,15,20-tetrakis(*N*-methylpyridinium-4-yl)porphyrin fully intercalates at 5'-CG-3' steps of duplex DNA in solution. *Biochemistry* **1999**, *38*, 15425–15437.
- (40) Anantha, N. A.; Azam, M.; Sheardy, R. D. Porphyrin binding to quadruplexed T₄G₄ DNA. *Biochemistry* **1998**, *37*, 2709–2714.
- (41) Wang, Y.; Patel, D. J. Solution structure of the human telomeric repeat d[AG₃(T₂AG₃)₃] G-tetraplex. *Structure* **1993**, *1*, 263–282.
- (42) Han, H.; Langley, D. R.; Rangan, A.; Hurley, L. H. Selective interaction of cationic porphyrins with G-quadruplex structures. *J. Am. Chem. Soc.* **2001**, *123*, 6485–6495.
- (43) Han, F. X.; Wheelhouse, R. T.; Hurley, L. H. Interaction of TMPyP4 and TMPyP2 with quadruplex DNA. Structural basis for the differential effects on telomerase inhibition. *J. Am. Chem. Soc.* **1999**, *121*, 3561–3570.
- (44) Haq, I.; Trent, J. O.; Chowdhry, B. Z.; Jenkins, T. C. Intercalative G-tetraplex stabilization of telomeric DNA by a cationic porphyrin. *J. Am. Chem. Soc.* **1999**, *121*, 1768–1779.
- (45) Adler, A. D.; Longo, F. R.; Finarelli, J. D.; Goldmacher, J.; Assour, J.; Korsakoff, L. A Simple synthesis for *meso*-tetraphenylporphyrin. *J. Org. Chem.* **1967**, *32*, 476.
- (46) Gunter, M. J.; Mander, L. N. Synthesis and atropisomer separation of porphyrins containing functionalization at the 5,15-*meso* positions: application to the synthesis of binuclear ligand systems. *J. Org. Chem.* **1981**, *46*, 4792–4795.
- (47) Ackerley, N.; Brewster, A. G.; Brown, G. R.; Clarke, D. S.; Foubister, A. J.; Griffin, S. J.; Hudson, J. A.; Smithers, M. J.; Whittamore, P. R. O. A Novel approach to dual-acting thromboxane receptor antagonist/synthase inhibitors based on the link of 1,3-dioxane-thromboxane receptor antagonists and thromboxane synthase inhibitors. *J. Med. Chem.* **1995**, *38*, 1608–1628.
- (48) Million, M.-E.; Mailliet, P.; Chen, H.; Bashiardes, G.; Boiziau, J.; Parker, F.; Commercon, A.; Tocque, B.; Roques, B. P.; Garbay, C. Synthesis and biological evaluation of a new series of phenylhydroquinone derivatives as new inhibitors of EGF-R-associated PTK activity. *Anti-Cancer Drug Des.* **1996**, *11*, 129–153.
- (49) Snyder, S. E.; Aviles-Garay, F. A.; Chakraborti, R.; Nichols, D. E.; Watts, V. J.; Mailman, R. B. Synthesis and evaluation of 6,7-dihydroxy-2,3,4,8,9,13*b*-hexahydro-1*H*-benzo[6,7]cyclohepta[1,2,3-*ef*][3]benzazepine, 6,7-dihydroxy-1,2,3,4,8,12*b*-hexahydroanthr[10,4a,4-*cd*]azepine, and 10-(aminomethyl)-9,10-dihydro-1,2-dihydroxyanthracene as conformationally restricted analogues of β -phenyldopamine. *J. Med. Chem.* **1995**, *38*, 2395–2409.
- (50) Clezy, P. S.; Smythe, G. A. The chemistry of pyrrolic compounds VIII. Dipyrrolylthiones. *Aust. J. Chem.* **1969**, *22*, 239–249.
- (51) Chong, R.; Clezy, P. S.; Liepa, A. J.; Nichol, A. W. The chemistry of pyrrolic compounds VII. Synthesis of 5,5'-diformyldipyrrolyl-methanes. *Aust. J. Chem.* **1969**, *22*, 229–238.
- (52) Mankra, J. S.; Lawrence, D. S. High yielding synthesis of 5,10-diarylporphyrins. *Tetrahedron Lett.* **1989**, *30*, 6989–6992.
- (53) Dancil, K.-P. S.; Hilario, L. F.; Khoury, R. G.; Mai, K. U.; Nguyen, C. K.; Weddle, K. S.; Shachter, A. M. Synthesis and aggregation of cationic porphyrins. *J. Heterocycl. Chem.* **1997**, *34*, 749–755.
- (54) Sun, D.; Hurley, L. H.; Von Hoff, D. D. Telomerase assay using biotinylated-primer extension and magnetic separation of the products. *BioTechniques* **1998**, *25*, 1046–1051.
- (55) Han, H.; Cliff, C. L.; Hurley, L. H. Accelerated assembly of G-quadruplex structures by a small molecule. *Biochemistry* **1999**, *38*, 6981–6986.
- (56) Cauzzo, G.; Gennari, G.; Jori, G.; Spikes, J. D. The Effect of chemical structure on the photosensitizing efficiencies of porphyrins. *Photochem. Photobiol.* **1977**, *25*, 389–395.
- (57) Georgiou, G. N.; Ahmet, M. T.; Houlton, A.; Silver, J.; Cherry, R. J. Measurement of the rate of uptake and subcellular localization of porphyrins in cells using fluorescence digital imaging microscopy. *Photochem. Photobiol.* **1994**, *59*, 419–422.
- (58) Villanueva, A.; Jori, G. Pharmacokinetic and tumor-photosensitizing properties of the cationic porphyrin *meso*-tetra(4*N*-methylpyridyl)porphine. *Cancer Lett.* **1993**, *73*, 59–64.
- (59) Izbicka, E.; Nishioka, D.; Marcell, V.; Raymond, E.; Davidson, K. K.; Lawrence, R. A.; Wheelhouse, R. T.; Hurley, L. H.; Wu, R. S.; Von Hoff, D. D. Telomere-interactive agents affect proliferation rates and induce chromosomal destabilisation in developing sea urchin embryos. *Anti-Cancer Drug Des.* **1999**, *14*, 355–365.
- (60) Still, W. C.; Khan, M.; Mitra, A. Rapid chromatographic technique for preparative separations with moderate resolution. *J. Org. Chem.* **1978**, *43*, 2923–2925.
- (61) Matsushima, Y.; Sugata, S.; Saionji, Y.; Tsutsui, M. *meso*-Tetra-[5-(8-hydroxyquinolyl)]porphine. A novel porphyrin with metal-chelating groups in the peripheral region. *Chem. Pharm. Bull.* **1980**, *28*, 2672–2675.
- (62) Boschelli, D. H.; Kramer, J. B.; Khatana, S. S.; Sorenson, R. J.; Conner, D. T.; Ferin, M. A.; Wright, C. D.; Lesch, M. E.; Imre, K.; Okonkwo, G. O.; Schrier, D. J.; Conroy, M. C.; Ferguson, E.; Woelle, J.; Saxena, U. Inhibition of E-selectin-, ICAM-1-, and VCAM-1-mediated cell adhesion by benzo[*b*]thiophene-, benzofuran-, indole-, and naphthalene-2-carboxamides: identification of PD 144795 as an anti-inflammatory agent. *J. Med. Chem.* **1995**, *38*, 4597–4614.

JM010246U